Materials Letters, Vol. 138, pp. 96-99 (2015).

κ-carbide hardening in a low-density high-Al high-Mn multiphase steel

W.J. Lu, X.F. Zhang, R.S. Qin*

Department of Materials, Imperial College London, Exhibition Road, London SW7 2AZ, United Kingdom

Abstract

κ-carbide hardening in a ferrite-austenite duplex low-density FeMnAlC steel has been investigated as a function of annealing processing within the temperature range 500−900 °C. Below 600 °C, a high hardness can be attained by the fine microstructures, e.g. the thin lamellar κ-carbides in austenite and dispersed nanosized particulate κ-carbides in ferrite. After further annealing, the alloy softened rapidly, and its hardness deteriorated drastically due to the formation of boundary κ-carbides composed of discontinuously coarsened κ-carbides and spheroidized κ-carbides. Interestingly, all κ-carbides within ferrite were transformed into austenite by the $\kappa+\alpha\rightarrow\gamma$ transformation at 800 °C, while the κ-carbides within austenite were dissolved at 900 °C. The κ-carbides are found to have a close to Nishiyama-Wasserman orientation relationship with the ferrite matrix.

Keywords: Lightweight steel; κ-carbide; Precipitation strengthening; Decomposition; *d*-spacing

*Corresponding authors. Tel.: +44 (0)20 7594 6803; fax: +44 (0)20 7594 6757. *E-mail addresses:* r.qin@imperial.ac.uk (R.S. Qin).

1. Introduction

Currently much further attention has been paid to lightweight steels having excellent combinations of specific strength and ductility due to the increasing demands for eco-friendliness and economic feasibility in transportation systems such as automobiles [1-4]. One of the most effective ways of reducing the weight is the addition of aluminium in steels to lower the density, which also enhances oxidation, corrosion resistance and impact toughness at high temperature [2-6]. These newly developed low-density steels can achieve tensile strengths above 780 MPa and elongations above 30% owing to precipitation strengthening of the κ-carbide, $(Fe,Mn)_3AlC$ [7]. Previously there are basically two variants of lightweight steels, austenite-based and ferrite-based steels, all of which can form thin lamellar κ-carbides with superior mechanical properties due to the suppression of microcrack initiation [8]. But the uncontrollable formation of boundary κ-carbides and spherical κ-carbide bands coarsening in ferrite matrix frequently induces cracking initiation and propagation [8-10]. Therefore, how to control the size, volume fraction and morphology of κ-carbides is the key factor to determine the mechanical properties of lightweight steels. In contrast to the amount of research devoted to the single-phase alloys, studies on multiphase steels are indeed rare although it possesses much better strength (above 1.0 GPa) and elongation (above 40%) [2,11-14]. Moreover, no systematically description and explanation have so far been made on the κ-carbides formation and its precipitation hardening under various annealing conditions in both austenite and ferrite simultaneously.

The present study aims at clarifying the correlation of precipitation hardening with microstructural evolution in the low-density multiphase steel. For this purpose, a ferrite-austenite duplex low-density Fe-26Mn-9Al-0.75C (wt.%) steel was subjected to various annealing treatments to produce κ-carbide precipitates with various sizes and volume fractions, and then Vickers hardness test was performed. The suitability of such materials for automotive applications is discussed based on the balance of structure and properties.

2. Material and experimental details

The steel with a chemical composition Fe-26Mn-9Al-0.75C (wt.%) used in this study was produced by an induction furnace. The density of the steel was measured by densitometry to be 6.47 g·cm^{-3}, which shows an apparent reduction of ～17% in comparison with transformation-induced plasticity or twinning induced plasticity steels when approximately 9 wt.% aluminium was added into the steels. The cast ingots were reheated to 1200 ^{o}C for 4h, hot-rolled from 30 mm to 3 mm in thickness at 1100 ^{o}C and water quenched. The hot-rolled steels were then rolled at room temperature to produce a 1 mm thick sheet. Subsequent annealing treatments were performed between 500 and 900 ^{o}C for 6h and water quenched. The Vickers hardness was measured by a tester under a 2 Kg load. Three dog-bone specimens treated at 600 ^{o}C with cross-section 1.5×1 mm^2 and gauge length 24 mm were used for tensile measurements. The strain rate is 10^{-3} s^{-1}. Detailed microstructural observations by scanning electron microscopy (SEM), electron backscatter diffraction (EBSD), transmission electron microscopy (TEM), and X-ray diffraction (XRD) were performed on the annealed samples at room temperature. Elemental partitioning in phases was calculated using Thermo-Calc software and was characterized by monitoring changes in the *d*-spacing values.

3. Results and discussion

SEM and EBSD micrographs show the microstructure evolutions of investigated steels within the temperature range 500−900 ^{o}C (Fig. 1). In the cold-rolled steel, two major phases consisting of austenite and ferrite existed in the matrix without any κ-carbides. But annealed at 500 ^{o}C, lamellar κ-carbides started to nucleate at the boundary of austenite (Fig. 1a). Simultaneously, particulate κ-carbides were observed in ferrite matrix (Fig. 1b). All dimensions of the nucleated κ-carbides (e.g. thickness of lamina and diameter of particle) were at the nanoscale. Subsequently, a large amount of lamellar κ-carbides were formed in austenite regions due to the decomposition of austenite ($\gamma \rightarrow \kappa + \alpha$) when the temperature reached 600 ^{o}C (Fig. 1c). Slight coarsening of particulate κ-carbides was also observed in ferrite matrix, but its size was still at nanoscale (Fig. 1d). The morphology of κ-carbides was significantly changed from lamellar to spherical shape within austenite at 700 ^{o}C due to the spheroidization of lamellar κ-carbides (Fig. 1e). Due to the partial dissolution of lamellar κ-carbides in austenite, the alloying elements of Al and Mn would contribute to the formation of boundary κ-carbides along ferrite boundaries (Fig. 1f). The size of particle in the inner part of ferrite reached to micron level (Fig. 1f). Interestingly, spherical κ-carbides within austenite were partially dissolved (Fig. 1g) at 800 ^{o}C, while all κ-carbides within ferrite were transformed into austenite (Fig. 1h). The inset in Fig. 1h collected by EBSD demonstrates the formation of austenite by the $\kappa+\alpha\rightarrow\gamma$ transformation. The formation of austenite (red phase) in the ferrite matrix (blue phase) indicates that the austenite becomes thermodynamically stable through the austenite forming temperature, and high contents of C and Mn should be supplied by the dissolution of κ-carbides for the formation of austenite. At 900 ^{o}C, all κ-carbides were dissolved and only ferrite and austenite remained in the steel.

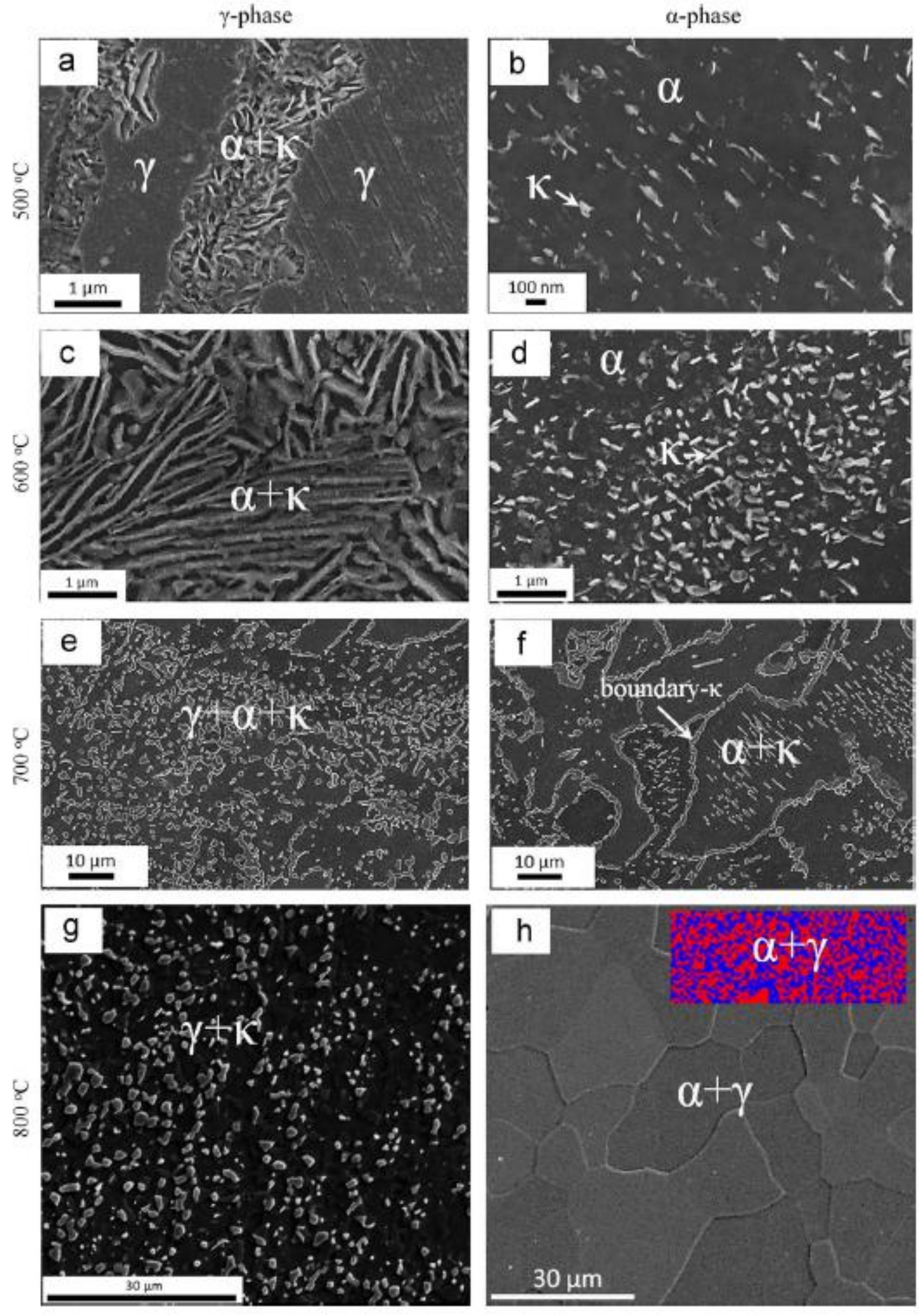

FIG. 1 SEM and EBSD micrographs illustrating the microstructural evolution in steels within the temperature range 500−800 ^{o}C.

TEM was performed to confirm the decomposition of austenite $\gamma \rightarrow \kappa + \alpha$ and the orientation relationship between κ-carbide and ferrite. Fig. 2 shows a TEM bright field image, selected area diffraction pattern and its corresponding schematic graph of diffraction pattern for the steel annealed at 600 ^{o}C. From the calculations of lattice parameter and crystal structure, the dark lamellar phase was determined to be κ-carbide with lattice parameter 3.75 Å, whereas the bright phase was ferrite with lattice parameter 2.92 Å. The diffraction pattern confirms a $(11\bar{1})_{\kappa} // (110)_{\alpha}$ and $[011]_{\kappa} // [001]_{\alpha}$ orientation relationship between ferrite and κ-carbide. This corresponds to the Nishiyama-Wasserman relationship, which is consistent with the previous reports [3,5,8]. Furthermore, the orientation relationship might be affected by the grain rotation and carbide spheroidization with increased annealing temperature. In addition, the retained austenite can also be observed in bright field image.

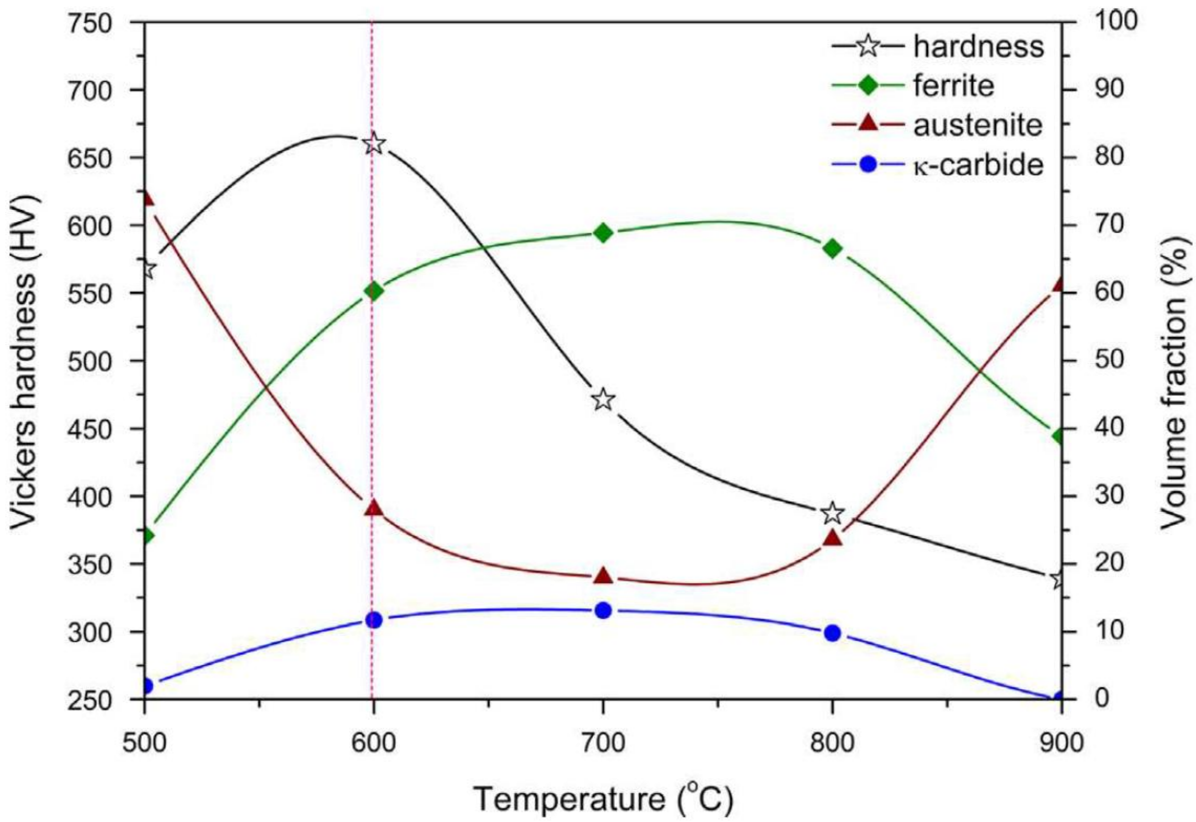

FIG. 2 Decomposition of austenite $\gamma \rightarrow \kappa + \alpha$ and the orientation relationship between κ-carbide and ferrite for the steel annealed at 600 °C were analysed by TEM. A TEM bright field image, selected area diffraction pattern and its corresponding schematic graph of diffraction pattern were illustrated.

The above-mentioned steels were detected by XRD to determine the fraction change of each phase with temperature. Vickers hardness of each state was also measured. The two groups of data were combined into a plot to clarify the correlation of microstructural evolution with precipitation hardening (Fig. 3). When the temperature was increased from 500 to 600 °C, the fraction of austenite started to decrease from 73.8 to 28.0 %, while both ferrite and κ-carbide increased to 28 and 11.7 %, respectively. This reduction of austenite indicated the decomposition of austenite $\gamma \rightarrow \kappa + \alpha$. For the hardness, it quickly rose to a maximum at 600 °C. The corresponding tensile strength at 600 °C was determined to be above 1.1 GPa according to the engineering stress-strain curve. It indicates that the fine lamellar κ-carbides in austenite and dispersed nanosized particulate κ-carbides in ferrite have great contributions to enhance the mechanical properties due to the suppression of microcrack initiation at fine carbides. But when temperature was above 600 °C, the alloy softened rapidly, and its hardness deteriorated drastically due to the formation of boundary κ-carbides composed of discontinuously coarsened κ-carbides and spheroidized κ-carbides. These particles frequently induced cracking initiation and propagation; accordingly they resulted in the deterioration of the mechanical properties. As temperature reached 900 °C, the volume fraction of κ-carbides decreased to minimum value, and the hardness also dropped to the lowest value.

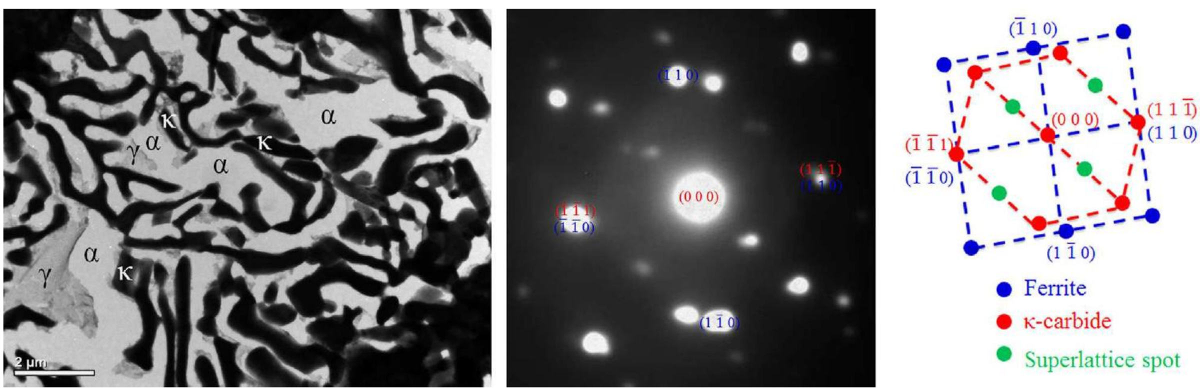

FIG. 3 The fraction change of each phase with temperature was determined by XRD. Vickers hardness of each state was also measured.

A plot calculated by Thermo-Calc software was used to predict the equilibrium concentration values of C, Al and Mn in austenite and ferrite as a function of temperature (Fig. 4a). Most of the C and Mn can be solved in austenite, but the measured partitioning ratio of austenite to ferrite at 500 ^{o}C is 0.7 for Al. Even though Al is a strong ferrite former, a considerable amount of Al is solved in austenite. Because the diffusion of C inside the austenite is fast, the nucleation of κ-carbide is controlled by segregation of C [5,10,13]. Thus, the high Al partitioning into austenite and fast diffusion of C greatly contribute to the nucleation of κ-carbide, leading to an accelerated decomposition of the austenite. Moreover, the nucleation of particulate κ-carbides in ferrite should be also induced by C diffusion and Al partitioning. As reported, the elemental partitioning in transformations can be detected from monitoring changes in the measured *d*-spacing values [15,16]. Fig. 4b shows the progression of the measured austenite (111) and ferrite (110) *d*-spacing values as a function of temperature. In the initial stages, the *d*-spacing values of austenite and ferrite display a steady decrease, which corresponds to lattice contraction due to κ-carbide precipitation. But *d*-spacing values of austenite and ferrite exhibit a sharp increase during continuous heating, indicating that κ-carbides begin to dissolve into the matrix (e.g. spheroidization and dissolution). These dissolved κ-carbides can provide more alloying elements (e.g. C and Mn) to promote the nucleation of austenite as continuously heating this steel. In addition, a 3-times relationship between yield strength and hardness value has been established by Ashy, Jones and Tabor [17]. Thus, the higher the hardness, the bigger the yield strength. Therefore, this type of new developed low-density multiphase steel consisting of thin lamellar κ-carbides in austenite and dispersed nanosized particulate κ-carbides in ferrite has a great potential application in the automobiles due to its superior mechanical properties.

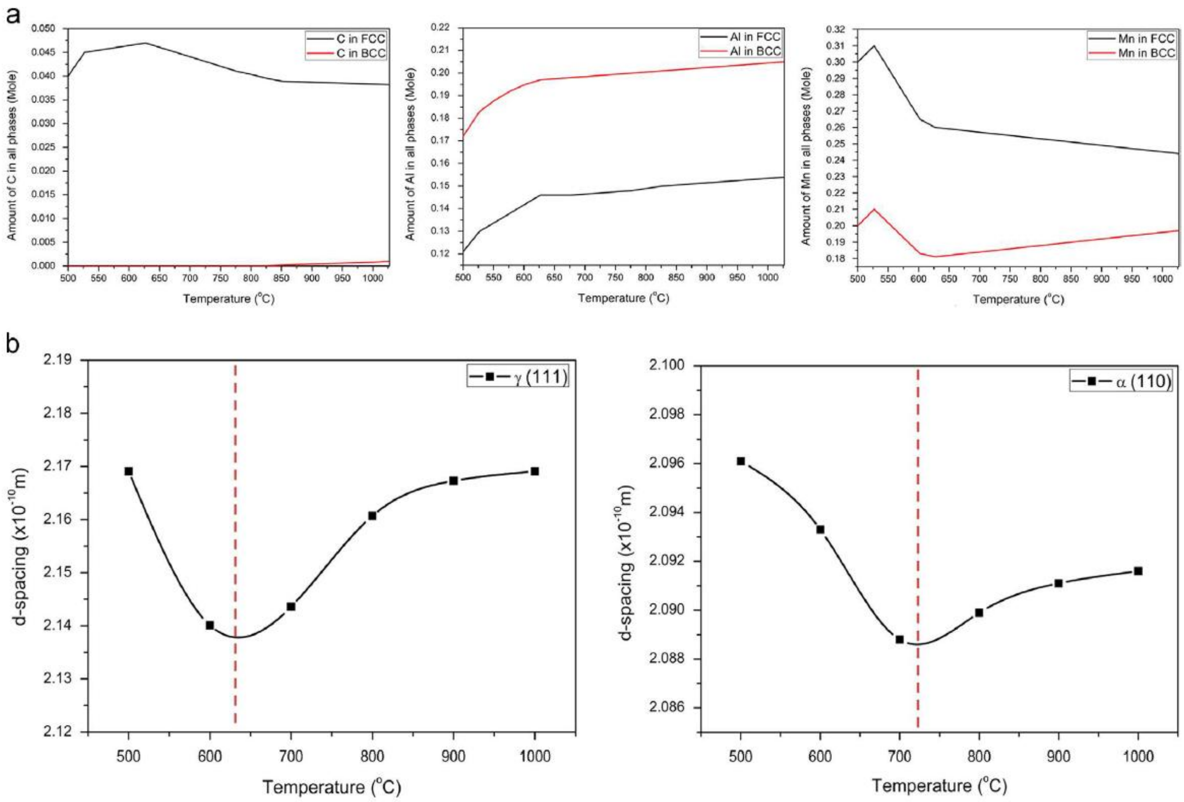

FIG. 4 (a) Calculated equilibrium concentration of C, Mn, and Al in ferrite and austenite by Thermo-Calc software. (b) The progression of the measured austenite (111) and ferrite (110) *d*-spacing values as a function of temperature.

4. Conclusions

Microstructural evolution and precipitation hardening had been systematically investigated in a Fe-26Mn-9Al-0.75C duplex lightweight steel within the temperature range 500−900 ^{o}C. Based on experimental observations and thermodynamic calculations, the following conclusions have been drawn.

1. The thin lamellar κ-carbides in austenite and dispersed nanosized particulate κ-carbides in ferrite nucleated firstly, which contributed significantly to precipitation hardening. But the formation of boundary κ-carbides and particulate κ-carbides coarsening in ferrite greatly deteriorated mechanical properties.

2. The precipitation, spheroidization and dissolution of κ-carbides are controlled by segregation of C and the high Al partitioning. Elemental partitioning for κ-carbides evolution can be detected from monitoring changes in the measured *d*-spacing values of austenite and

ferrite. As the temperature increases, both *d*-spacing values of austenite and ferrite exhibit a steady decrease firstly due to κ-carbide precipitation, and then a sharp increase during continuous heating resulted by the spheroidization and dissolution of κ-carbides.

3. Interestingly, all κ-carbides within ferrite were transformed into austenite by the $\kappa+\alpha\rightarrow\gamma$ transformation at 800 ^{o}C, while the κ-carbides within austenite were dissolved at 900 ^{o}C. The κ-carbides are found to have a close to Nishiyama-Wasserman orientation relationship with the ferrite matrix.

Acknowledgement

The authors gratefully acknowledge the financial support from TATA Steel, Royal Academy of Engineering and EPSRC (No. EP/J011460/1) at United Kingdom.

References

[1] Wang TP, Kao FH, Wang SH, Yang JR, Huang CY, Chen HR. Mater Lett 2011;65:396−9.

[2] Rana R, Liu C, Ray RK. Scripta Mater 2013;68:354−9.

[3] Sohn SS, Lee BJ, Lee S, Kim NJ, Kwak JH. Acta Mater 2013;61:5050−66.

[4] Gutierrez-Urrutia I, Raabe D. Scripta Mater 2013;68:343−7.

[5] Seol JB, Raabe D, Choi P, Park HS, Kwak JH, Park CG. Scripta Mater 2013;68:348−53.

[6] Chen PC, Chao CG, Liu TF. Scripta Mater 2013;68:380−3.

[7] Choo WK, Kim JH, Yoon JC. Acta Mater 1997;45:4877−85.

[8] Han SY, Shin SY, Lee S, Kim NJ, Kwak JH, Chin KG. Metall Mater Trans A 2011;42:138−46.

[9] Sohn SS, Lee BJ, Lee S, Kwak JH. Acta Mater 2013;61:5626−35.

[10] Shin SY, Lee H, Han SY, Seo CH, Choi K, Lee S, Kim NJ, Kwak JH, Chin KG. Metall Mater Trans A 2010;41:138−48.

[11] Frommeyer G, Brüx U. Steel Res Int 2006;77:627−33.

[12] Yi HL, Chen P, Hou ZY, Hong N, Cai HL, Xu YB, Wu D, Wang GD. Scripta Mater 2013;68:370−4.

[13] Kim H, Suh DW, Kim NJ. Sci Technol Adv Mater 2013;14:1−11.

[14] Sutou Y, Kamiya N, Umino R, Ohnuma L, Ishida K. ISIJ Int 2010;50:680-6.

[15] Terasaki H, Komizo Y. Scripta Mater 2011;64:29−32.

[16] Zhang XF, Terasaki H, Komizo Y. Scripta Mater 2012;67:201−4.

[17] Ashby MF, Jones DRH. Engineering materials. Oxford: Pergamon Press; 1980.